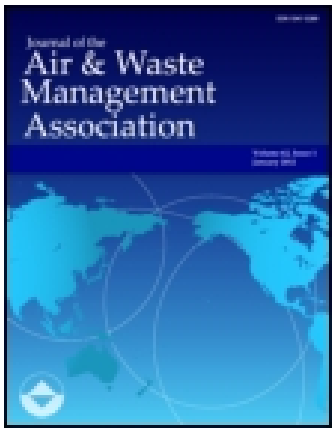

Journal of the Air & Waste Management Association
Publication details, including instructions for authors and subscription information:
http://www.tandfonline.com/loi/uawm20

Sensitivity and linearity analysis of ozone in East Asia: The effects of domestic emission and intercontinental transport

Joshua S. Fu [a], Xinyi Dong [a], Yang Gao [a], David C. Wong [b] & Yun Fat Lam [c]

[a] Department of Civil and Environmental Engineering, The University of Tennessee, Knoxville, TN, U.S.A

[b] Atmospheric Modeling and Analysis Division, US Environmental Protection Agency, Research Triangle Park, NC, U.S.A

[c] School of Energy and Environment, City University of Hong Kong, Hong Kong

Accepted author version posted online: 02 Jul 2012.Published online: 21 Aug 2012.

To cite this article: Joshua S. Fu, Xinyi Dong, Yang Gao, David C. Wong & Yun Fat Lam (2012) Sensitivity and linearity analysis of ozone in East Asia: The effects of domestic emission and intercontinental transport, Journal of the Air & Waste Management Association, 62:9, 1102-1114, DOI: 10.1080/10962247.2012.699014

To link to this article: http://dx.doi.org/10.1080/10962247.2012.699014

TECHNICAL PAPER

Sensitivity and linearity analysis of ozone in East Asia: The effects of domestic emission and intercontinental transport

Joshua S. Fu,[1,*] Xinyi Dong,[1] Yang Gao,[1] David C. Wong,[2] and Yun Fat Lam[3]
[1]*Department of Civil and Environmental Engineering, The University of Tennessee, Knoxville, TN, U.S.A*
[2]*Atmospheric Modeling and Analysis Division, US Environmental Protection Agency, Research Triangle Park, NC, U.S.A*
[3]*School of Energy and Environment, City University of Hong Kong, Hong Kong*
[*]*Please address correspondence to: Joshua S. Fu, Department of Civil and Environmental Engineering, The University of Tennessee, 223 Perkins Hall, Knoxville, TN, 37996, USA; e-mail: jsfu@utk.edu*

In this study, ozone (O_3) sensitivity and linearity over East Asia (EA) and seven urban areas are examined with an integrated air quality modeling system under two categories of scenarios: (1) The effects of domestic emission are estimated under local emission reduction scenarios, as anthropogenic NOx and volatile organic compounds (VOC) emissions are reduced by 20%, 50%, and 100%, respectively and independently; and (2) the influence of intercontinental transport is evaluated under Task Force on Hemispheric Transport of Air Pollution (TF HTAP) emission reduction scenarios, as anthropogenic NOx emission is reduced by 20% in Europe (EU), North America (NA), and South Asia (SA), respectively. Simulations are conducted for January and July 2001 to examine seasonal variation. Through the domestic O_3 sensitivity investigation, we find O_3 sensitivity varies dynamically depending on both time and location: North EA is VOC limited in January and NOx limited in July, except for the urban areas Beijing, Shanghai, Tokyo, and Seoul, which are VOC limited in both months; south EA is NOx limited in both January and July, except for the urban areas Taipei, which is VOC-limited in both months, and Pearl River Delta, which is VOC limited in January. Surface O_3 change is found to be affected more by NOx than by VOC over EA in both January and July. We also find different O_3 linearity characteristics among urban areas in EA: O_3 at Beijing, Tokyo, and Seoul shows a strong negative linear response to NOx emission in January; O_3 at Shanghai, Pearl River Delta, and Taipei shows a strong positive response to VOC emission in both January and July. Through the long-range transport investigation, monthly O_3 changes over EA resulting from different source regions indicate the largest source contribution comes from NA (0.23 ppb), followed by SA (0.11 ppb) and EU (0.10 ppb). All of the three regions show higher impacts in January than in July.

Implications: This study examine O_3 sensitivities and linear response of NOx and VOC emission over EA and seven urban areas based on regional air quality modeling system MM5/CMAQ. We also quantify the intercontinental transport effect from EU, SA, and NA over EA. The result provide a theoretical basis for emission control strategy design in EA, and also reveal the O_3 special nonlinearity features for further related studies that are applicable to other continents. The HTAP multimodel experiments need to examine the potential impacts on ground-level O_3 of changes in meteorology and transport patterns expected as a result of the regional scale.

Introduction

One of the most significant criteria pollutants affecting human health and ecosystems, tropospheric ozone (O_3) is formed through a sequence of chemical reactions involving volatile organic compounds (VOC), methane (CH_4), and carbon monoxide (CO) in the presence of nitrogen oxides (NOx) and sunlight (National Research Council, 1991). Excessive regional anthropogenic emissions of VOC and NOx may amplify or restrain the photochemical production of O_3 formation, depending on the VOC/NOx ratio (Liu et al., 2004; So et al., 2003; Wang et al., 2005). Therefore, it is essential to identify VOC-limited and NOx-limited regimes to provide scientific basis to support development of effective O_3 control strategies for regional air quality improvement. While the O_3–NOx–VOC relationship has been extensively studied in the United States (Jacob et al., 1995; Sillman, 1995; Sillman, 1999; Sillmand and He, 2002), much less attention has been paid to East Asia (EA). In a 2000 study conducted by Luo et al. (2000) with local anthropogenic emission of VOC and NOx reduced by 35%, it was found that in wintertime rural areas in south China are NOx limited, while rural areas in north China are more likely to be VOC limited. Model simulations from Wang et al. (2005) indicate that urban areas in the Pearl River Delta (PRD) region are VOC limited in March, while nonurban areas in PRD are NOx limited. These reported O_3 sensitivity features, however, are limited to specific seasons or local areas, which may not be applicable, for instance, for summertime's higher temperatures and more intensive photochemical activities, or appropriate for describing the O_3 sensitivity over whole EA domain. In addition, none of these studies provide a comprehensive investigation of the seasonal variation of ozone

Journal of the Air & Waste Management Association, 62(9):1102–1114, 2012. ISSN: 1096-2247 print
DOI: 10.1080/10962247.2012.699014

over EA. To achieve better air quality, it is important to investigate the characteristics of the O_3–VOC–NOx photochemical relationships (Hakami et al., 2004) and its seasonality on a regional scale (Cohan et al., 2006) over EA. Additionally, although the dependence of O_3 production on domestic NOx and VOC over the United States is strongly nonlinear based on a number of previous studies (Sillman, 1999; Jacob et al., 1995), very few studies have been conducted over EA. Xu et al. (2008) reported the long-term linear trend of maximum O_3 concentration from a regional background observational station in China relevant to NOx emission, but this study was limited to the rural site and did not consider VOC emission. Xing et al. (2011) recently conducted simulations over eastern China to characterize the NOx and VOC emission impacts on O_3, reported the nonlinear response of O_3 regarding to local and regional emissions, but only focused on O_3 isopleths for three cities. Yamaji et al. (2012) conducted a modeling study of O_3 response in Japan by controlling anthropogenic emission in China from −100 to +100%, and found a strong linear response in spring and summer over the range between −30 and +100% emission changes, but the finding is based on subdomain averaged values and may not be applicable for urban areas.

While local VOC and NOx emissions play an important role in O_3 formation, intercontinental transport may also affect the background O_3 significantly in downwind regions (Bernsten et al., 1999; Fiore et al., 2002; Heald et al., 2006; Wu et al., 2009). In order to evaluate the long-range transport effects of air pollutants and source–receptor (SR) relationships for O_3 in the Northern Hemisphere, the Task Force on Hemispheric Transport of Air Pollution (TF HTAP) was established under the United Nations Economic Commission for Europe (UNECE) Convention on Long-Range Transboundary Air Pollution (LRTAP). Applying 21 global chemical transport models (CTMs), Fiore et al. (2009) reported the monthly ensemble mean O_3 changes from 21 global model outputs for all SR scenarios. Although these global CTMs provide an essential broad outline to estimate the intercontinental SR relationships, it is reported that there are significant uncertainties regarding the representation of both chemical mechanisms (Emmerson and Evans 2009) and physical parameterizations due to the global-scale spatial resolution of 2° × 2.5° or coarser. Moreover, since rapid industrialization over EA has introduced large amounts of anthropogenic emissions of air pollutants and precursors (Streets et al., 2003; Streets et al., 2007) within the recent decade, most of the studies focus on EA as a major source region for air pollutants (Jaffe et al., 1999; Jacob et al., 1999). Much less attention has been paid concerning the impacts from other continents on EA, which could also suffer as a receptor region from long-range transport of air pollutants from Europe (EU), North America (NA), and South America (SA) (Fiore et al., 2009; Holloway et al., 2008). Fu et al. (2011) reported SA could contribute 8–18 ppbv on O_3 over southeastern EA in the biomass burning period; Holloway et al. (2008) found that EU and NA emissions contribute up to 9 ppbv of O_3 over western Mongolia in summer, and 5–7 ppbv over Japan in the spring and late fall, based on results from global Model of Ozone and Related Tracers (MOZART). These studies imply the significance of intercontinental transport effects over EA, but still lack detailed information about SR relationships regarding EA in different seasons. Likewise, they may retain uncertainties from the global model.

We have undertaken this study to conduct a regional modeling assessment and long range transport analysis by applying the fifth-generation Mesoscale Model version/Community Multiscale Air Quality (MM5/CMAQ) modeling system over EA for two reasons: (1) to link O_3 sensitivities and linearity with local VOC and NOx emissions in EA for both winter and summer, and (2) to quantify the impacts from EU, NA, and SA on surface O_3 concentration in EA at a finer-scale resolution under TF HTAP scenarios, and examine its relative importance compared with domestic emissions. We also select seven urban areas of most air pollution concern within the EA domain because of their condensed population and developed economic and industries. This is the first attempt to model O_3 in different seasons under both domestic and intercontinental transport emission removal scenarios to characterize the O_3 sensitivity features and linearity of O_3 responses to local NOx and VOC emission change, and also to quantify the long-range transport effects spread over EA, as well as the impacts in urban areas.

Methods

Model configuration

CMAQ is a regional air quality model developed by the U.S. Environmental Protection Agency (EPA) (Byun and Schere, 2006; Byun and Ching, 1999). It has been applied in numerous governmental and research studies for making regulatory decisions and conducting scientific atmospheric research in the United States. In our study, CMAQv4.6 is driven by meteorological fields from MM5 version 3.6. Model configurations are listed in Table 1. The National Centers for Environmental Prediction (NCEP) Final Analyses Data (ds083.2) with a spatial resolution of 1.0 × 1.0° and a 6-hourly temporal resolution was used to drive the MM5 model, along with 6-hourly observational data including NCEP Automated Data Processing (ADP), surface observations data set (ds464.0), and upper air observations (ds353.4). The one-way nested approach with four-dimensional data assimilation (FDDA) in MM5 was performed from a mother domain with a 108 km × 108 km horizontal resolution (ranging from 174 to 46° E, 3 to 65° N) over Asia nest-down to 36 km × 36 km (72.5–147° E, 15–49.5° N). Meteorology/Chemistry Interface Processor (MCIP) 2.3 (Byun and Schere 2006) was used to process MM5 output, and the outcome was used as the input for CMAQ.

The emission inventory in this study for CMAQ was developed from the Transport and Chemical Evolution over the Pacific (TRACE-P) project, which has been successfully applied and validated in other Asia-related studies (Streets et al., 2003, 2007; Fu et al., 2009). Eleven major chemical species were involved in the TRACE-P emission inventory, including gas-phase species such as methane (CH_4), carbon dioxide (CO_2), sulfur dioxide (SO_2), NOx, carbon monoxide (CO), ammonia (NH_3), nonmethane volatile organic compounds (NMVOC), particulate matter with aerodynamic diameter less than or equal to 2.5 μm

Table 1. Model configurations for MM5 and CMAQ

MM5 configuration	
Vertical resolution	34 σ_p levels
Horizontal resolution	36 km
Projection	Lamber conformal
FDDA	Analysis nudging
Cumulus	Kain–Fritsch (Kain and Fritsch, 1993)
Microphysics	Mixed phase
Radiation	RRTM
PBL	Pleim–Xiu
LSM	Pleim–Xiu LSM
LULC	USGS 25-category
CMAQ configuration	
Horizontal resolution	36 km
Vertical resolution	14 sigma-pressure levels (with the top pressure of 100 mb)
Projection	Lambert conformal conic
Depth of first later	36 m
Advection	Piecewise parabolic scheme
Vertical diffusion	K-theory
Gas-phase chemistry	CB-IV with EBI solver
Dry deposition	Wesely (Wesely, 1989)
Wet deposition	Henry's law
Aqueous chemistry	Walcek (Walcek and Aleksic, 1998)
Advection	Global mass-conserving scheme
PBL scheme	Blackadar (Zhang and Anthes, 1982)
Explicit moisture scheme	Mixed phase (Reisner et al., 1998)
Atmospheric radiation scheme	Cloud (Dudhia, 1993)
Cumulus scheme	Grell
Multilayer soil temperature model	Five-layer soil model

($PM_{2.5}$), PM_{10}, black carbon aerosol (BC), and organic carbon aerosol (OC) (Streets et al., 2003; Woo et al., 2002). NMVOC emissions were further speciated into 19 subcategories based on chemical reactivity and functional groups. The main anthropogenic emission sources were categorized according to five types of fossil fuels, which included power plants, industry, residential, transportation, and agricultural emissions. Biomass burning was evaluated independently in three major categories: the burning of forest, savanna/grassland, and crop residues. Biogenic emissions, such as isoprene and terpene emissions, were prepared by a geographic information system (GIS) based on Global Emissions Inventory Activity (GEIA; www.geiacenter.org) and land-use data. Due to the compatibility between TRACE-P chemical species and the Carbon Bond CB05 chemical species in CMAQ, mapping tables were developed to convert TRACE-P emissions into CB05 emissions, described in Fu et al. (2009).

Simulation scenarios

Initial and boundary (IC/BC) conditions of CMAQ were derived from GEOS-Chem, one of the 21 CTMs used in TF HTAP and also used in U.S. EPA regulatory modeling. GEOS-Chem incorporated various emission inventories for different sectors, such as using the Emission Database for Global Atmospheric Research (EDGAR) for anthropogenic emission, Model of Emissions of Gases and Aerosols from Nature (MEGAN) for biogenic emission, and Global Fire Emissions Database (GFED) for biomass burning emissions. Simulation results from GEOS-Chem were downscaled to transfer the intercontinental transport information of SR relationships from global scale to the regional scale in CMAQ. The downscaling methodology of IC/BC from GEOS-Chem to CMAQ has been described in Lam and Fu (2009, 2010).

GEOS-Chem output with 2001 original emissions was downscaled to produce IC/BC for the base scenario, which is denoted as SR1 hereafter. For local NOx and VOC reduction scenarios, SR1 IC/BC is the unchanged base case. O_3 sensitivity analyses were conducted under 20%, 50%, and 100% local anthropogenic emission reduction of NOx and VOC, respectively. For long-range transport scenarios, IC/BC was downscaled from GEOS-Chem outputs from three HTAP emission control scenarios: (1) 20% anthropogenic NOx emission reduction from Europe (SR3EU), (2) 20% reduction from North America (SR3NA), and (3) 20% reduction from South Asia (SR3SA).

January and July 2001 were selected as simulation periods for all of the sensitivity scenarios to characterize the O_3 seasonal variation over EA, and to examine the impacts from different seasonal monsoons, that is, the cold and dry winter monsoon and the warm and wet summer monsoon (Lin et al., 2008). Unlike surface ozone in the United States where summer ozone is of the major concern, winter ozone over EA is also of interest because it may be close to summer peak values. It has been reported by Li et al. (2011) that wintertime ozone (0.052 mg/m^3) in Shanghai is close to that in summer (0.054 mg/m^3), and Zhang et al. (2011) reported surface ozone at 10 observation sites in Pearl River Delta all peak in October. So it is necessary to examine the seasonality of ozone in EA.

Since it has been reported that European emissions exerted the most significant impacts on northern Asia (Holloway et al., 2008), three megacities—Beijing (BJ), Tokyo, and Seoul—in the north part of EA are selected, along with four urban areas in the south part of EA: Chengdu (CD), Pearl River Delta (PRD), Taiwan, and Shanghai (SH). These are the most developed urban areas in EA since they sustain concentrated populations and substantive anthropogenic emissions. The CMAQ model simulation is performed from December 23, 2000, to January 31, 2001, in winter, and from June 22, 2001, to July 31, 2001, in summer. The first few days of the simulation periods (December 23 to 31, 2000, and June 22 to 30, 2001) serve as spinning off days to protect against inappropriate initializations. Simulation results from January 1–31 and July 1–31, 2001, are used for analysis. The full simulation domain is shown in Figure 1, including most of the East Asian regions: China, Japan, North Korea, South Korea, Taiwan, and parts of Laos, Myanmar, and Vietnam.

MM5/CMAQ model evaluation

It is essential to evaluate models with observations to demonstrate credibility of model results. GEOS-Chem model

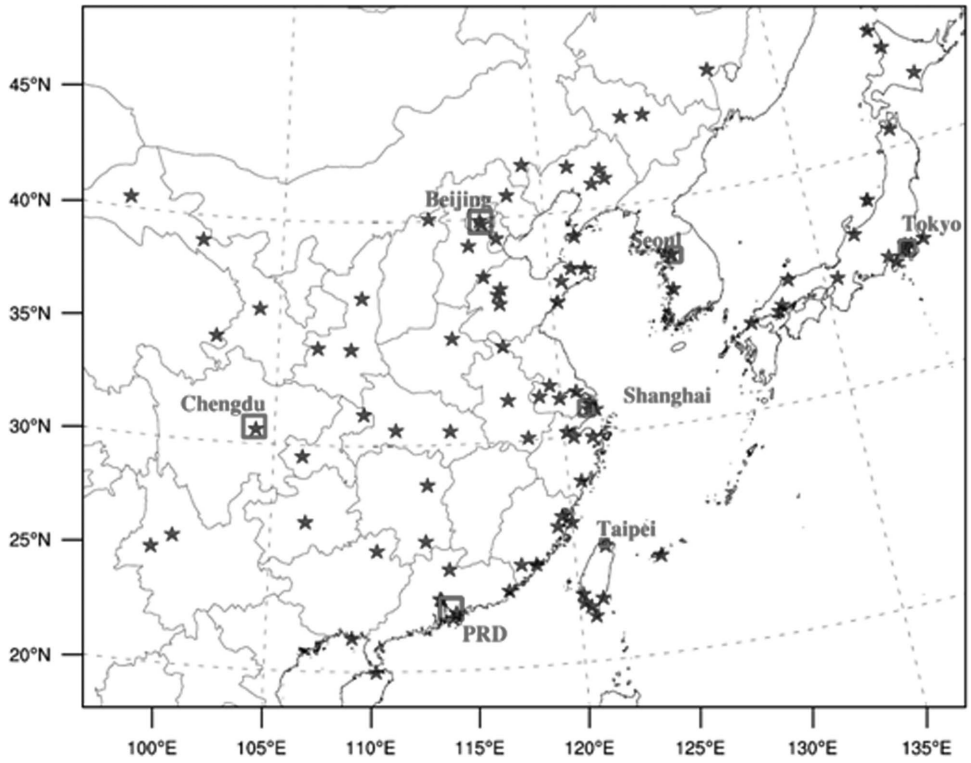

Figure 1. Model domain for the application of CMAQ in East Asia.

performance under TF HTAP scenarios has been evaluated in previous studies (Fiore et al., 2009). Thus, in this study, we evaluate the model with surface observations from National Climate Data Center (NCDC) for the MM5 meteorological field, and the Acid Deposition Monitoring Network (EANET) for CMAQ simulated surface O_3 in East Asia. Locations of the observational sites are shown in Figure 1.

We compare the evaluation results with the established statistical benchmarks (BM) for MM5 evaluation used by Kim et al (Kim et al., 2010) to demonstrate the credibility of MM5 performance in this study, as shown in Table 2.

According to very limited surface observational data over EA, we perform CMAQ model evaluations with hourly data at Taipei for O_3 and NOx, as shown in Figure 2. CMAQ generally performs well but underestimates NOx and overestimate O_3 in both January and July. Large negative biases of NOx may be mainly due to underestimated emissions, as indicated in Streets et al. (2003). In order to better determine the reason for overestimation of O_3, we performed statistical analysis by separating the daytime O_3 and nighttime O_3. Daytime O_3 has a much smaller bias (9.3 in January, 0.19 in July) than nighttime O_3 (16.02 in January, 9.38 in July), indicating the model overestimation of O_3 may be mainly due to the underestimation of NOx, which usually has a strong titration effect during the night time, especially in the most populated yet polluted urban areas in EA.

Results and Discussion

Seasonal variation of surface O_3 over EA

It has been recognized that surface O_3 distribution is closely related to meteorological conditions, and that wind patterns and temperature are the most important factors (Dawson et al., 2007). EA is greatly affected by monsoons in both winter and summer.

Table 2. Model evaluation for MM5

	Wind speed (m/s)			Wind direction (degree)			Temperature (K)		
	BM	JAN	JUL	BM	JAN	JUL	BM	JAN	JUL
RMSE	≤ 2	2.18	2.17						
Bias	≤ 0.5	0.19	0.06	≤ 10	6.68	0.4	≤ 0.5	0.98	0.68
Gross error				≤ 0	52.39	49.35	≤ 2	2.56	2.18
IOA	≥ 0.6	0.60	0.62				≥ 0.8	0.96	0.83

Note: RMSE: root mean square error. IOA: index of agreement (Willmont, 1981).

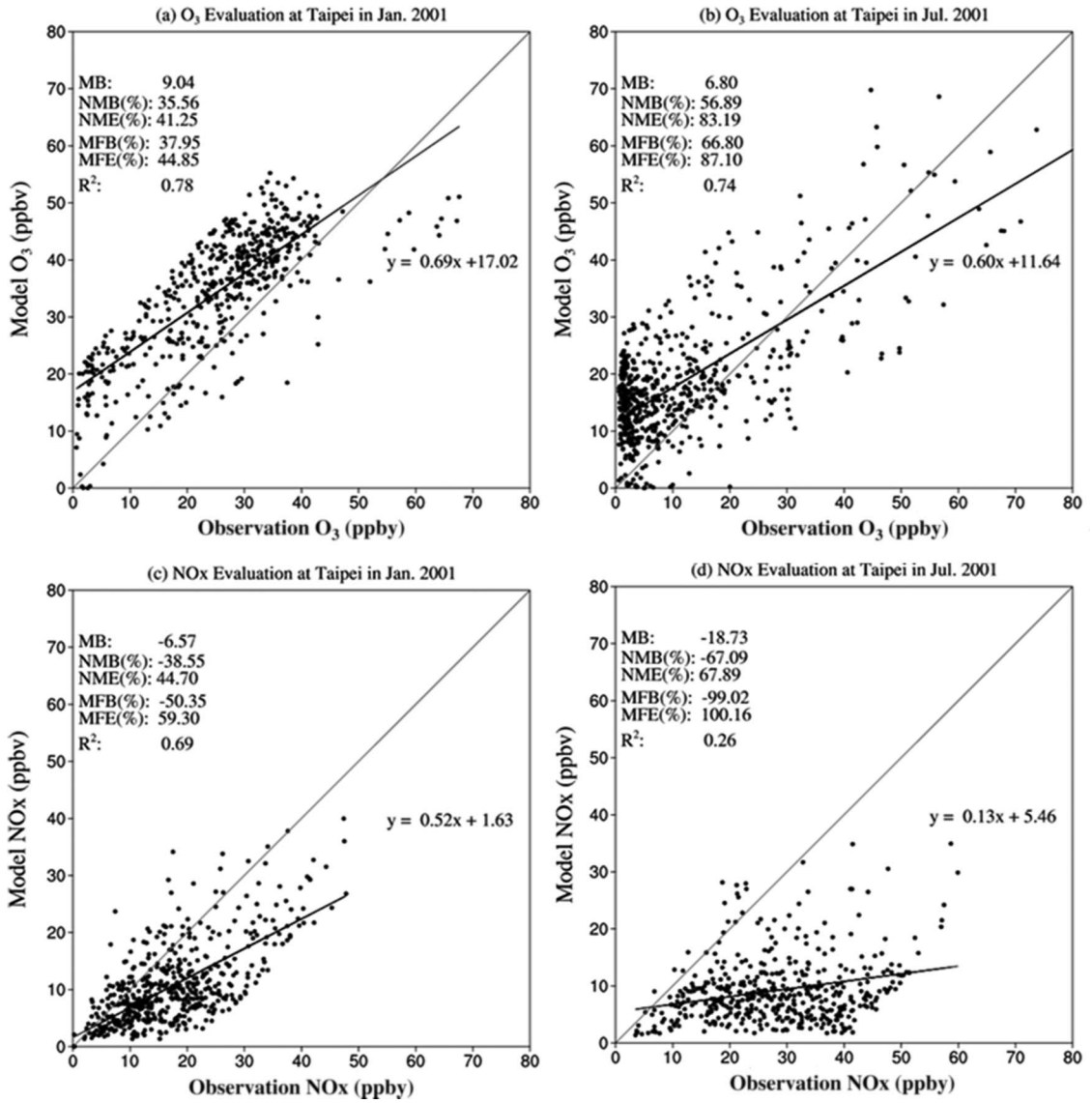

Figure 2. CMAQ model simulations evaluate against surface observations at Taipei for O_3 (first row) and NOx (second row) in January (left column) and July (right column), 2001.

In fact, this is one of the major controlling mechanisms affecting the spatial distribution of EA surface O_3. Temperature also varies greatly between winter and summertime for EA. Thus, the combined effects from the temperature gradient and wind patterns lead to different spatial patterns of surface O_3 in January and July. As shown in Figure 3, (a) and (b) illustrate the spatial distribution of monthly average wind and temperature from MM5; (c) and (d) show the monthly average O_3 from CMAQ. In January, temperature decreases gradually from around 300 K in the southern region of EA to 250 K in the northern region. During the same period, a Siberian high-pressure system drives air from northern China southeastward. Pollution contained in this air mass is the result of extensive utilization of coal for heating within this region. The temperature gradient and southeastward wind lead to lower O_3 due to weak photochemical production in the north part of EA, and a higher O_3 in the south part due to downstream pollution from the upper latitudes, especially along the east coast of China, where surface O_3 gradually increases from north to south. In July, temperature is almost within the same scale (around 300 K) for most areas of EA, resulting in similar photochemical production rates for O_3 in the north and south part. In summer, an intensified North Pacific high-pressure system expands westward and leads to the southeast summer monsoon in EA. Along with the northeastward SA summer monsoon coming from the Indian Ocean, the prevailing monsoon brings a clean marine air mass, and leads to the gradually increasing pattern of O_3 from south to north over EA. In addition, titration resulting from high emission of NOx and low emission of VOC is another important factor in determining ozone concentration in the northern part of EA especially in winter. As demonstrated in Figure 3c, the most populated areas including BJ and SH actually have the lowest ozone concentration, indicating a VOC-limited sensitivity case in these areas. We continue this discussion in the next subsection.

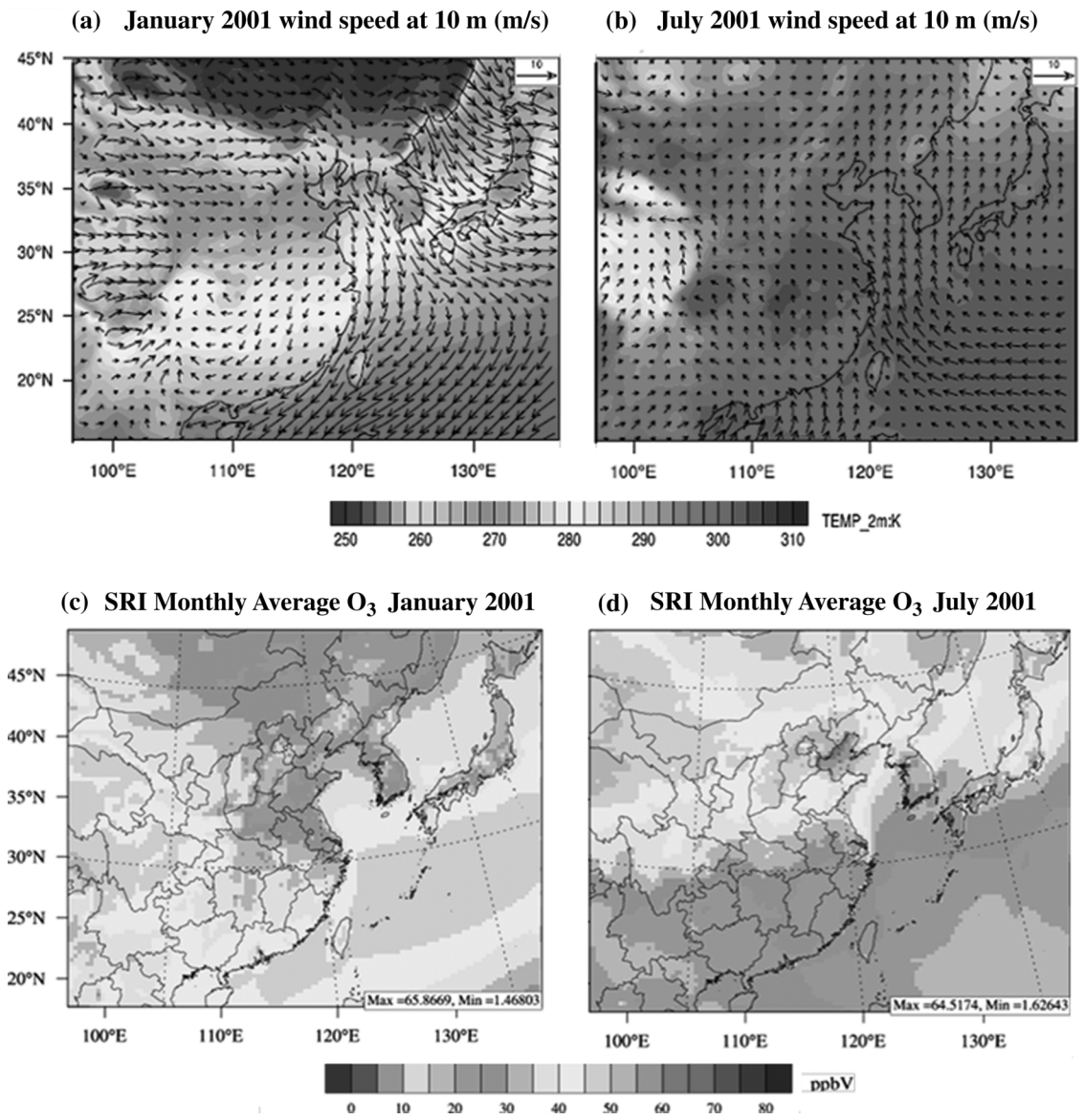

Figure 3. (a) Monthly mean wind speed, wind directions, and temperature in January and (b) July 2001. (c) Monthly mean hourly O_3 spatial distribution in January and (d) July 2001.

Analysis of O_3 sensitivity and linearity

In addition to meteorological conditions, chemical production is another dominant mechanism determining surface O_3 concentration, which is mainly affected by precursors including NOx and VOC. Figure 4 illustrates the O_3 changes over EA as a result of emission reduction of NOx or VOC under different control scenarios, which shows the contributions of NOx and VOC in O_3 production over different areas of EA.

As shown in Figure 4, in January, urban areas including Japan, South Korea, northeastern China, Yangtze River Delta, and PRD have O_3 concentration increased by up to 28.88 ppbv under the 100% NOx emission reduction scenario, and decreased by up to 12.52 ppbv under the 100% VOC emission reduction scenario, indicating a VOC-limited feature over these areas. This is consistent with our expectation, since most of the developed industries and heavy transportations are distributed within the areas just mentioned, and have an extensive amount of NOx emission. On the other hand, vegetation coverage is relatively lower in those areas compared to the south part of EA, which provides limited VOC emission especially in the wintertime. The other areas of EA are NOx limited due to a large amount of VOC emission from vegetation and less NOx emission from industry activities and vehicles. In July, as shown in Figures 4g to 4l, most of the areas that are VOC limited in January change to being NOx limited, due to the significantly increased amount of VOC emission from vegetation in the summertime in these mid-latitude regions. However, some large metropolitan areas, including BJ, SH, TP, Tokyo, and Seoul, remain VOC limited due to the extensive amount of NOx emission from vehicles and industries in the summer time.

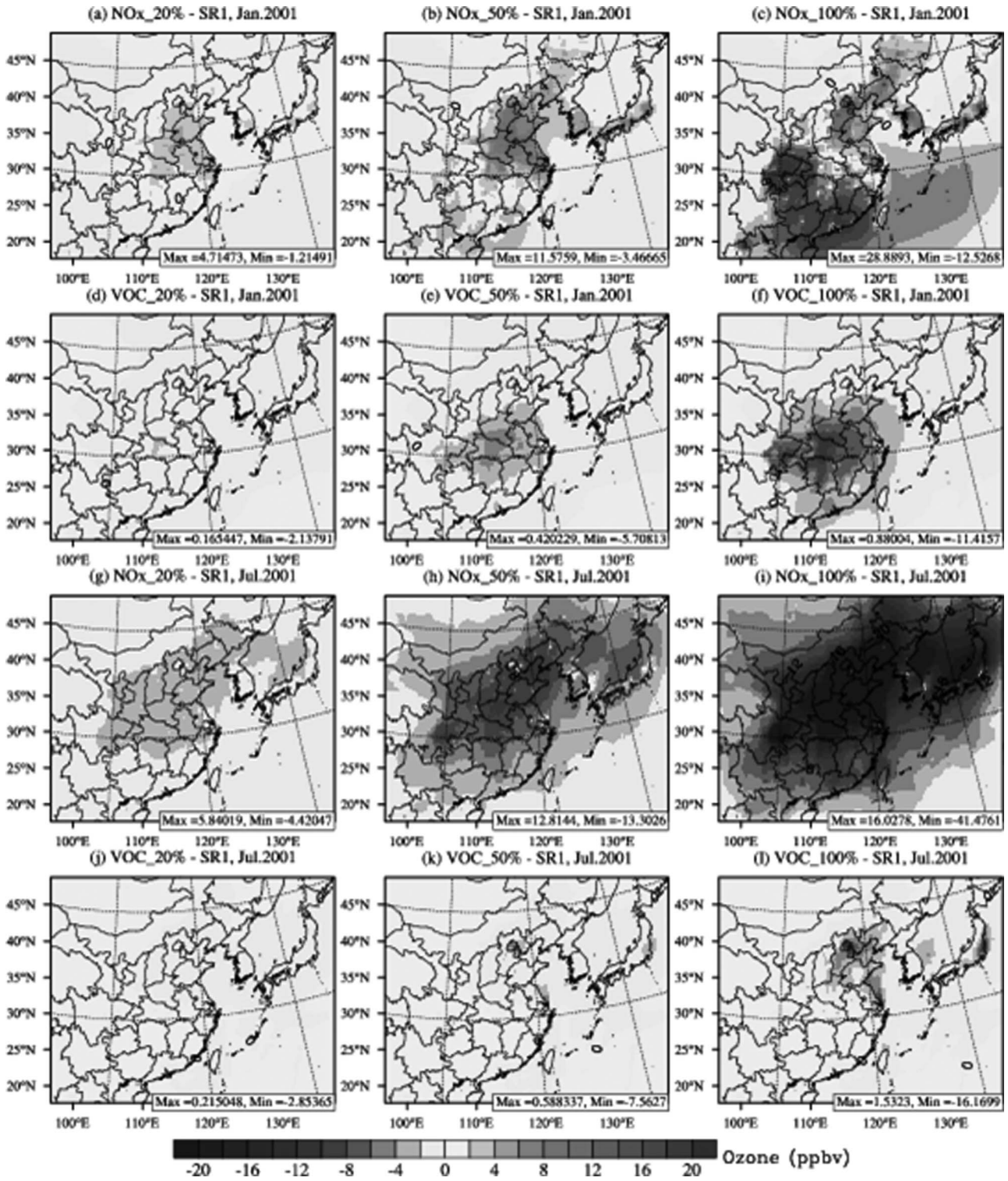

Figure 4. Spatial distribution of monthly average O_3 responses to local NOx emission reduction at rate of (a) 20%, (b) 50%, and (c) 100% in January, and (g) 20%, (h) 50%, and (i) 100% in July 2001; and the O_3 responses to VOC emission reduction at rate of (d) 20%, (e) 50%, and (f) 100% in January, and (j) 20%, (k) 50%, and (l) 100% in July 2001.

In January, NOx reduction scenarios show a more beneficial effect on the surface concentration of O_3 in the south part of EA, while VOC reductions are more beneficial in the north part. In July, NOx reduction is beneficial for almost the whole EA. In order to reveal the features of O_3 sensitivity and linear (or non-linear) response in the major urban areas as well as whole EA domain, we further analyze the O_3 concentration changes for these areas as demonstrated in Figure 5.

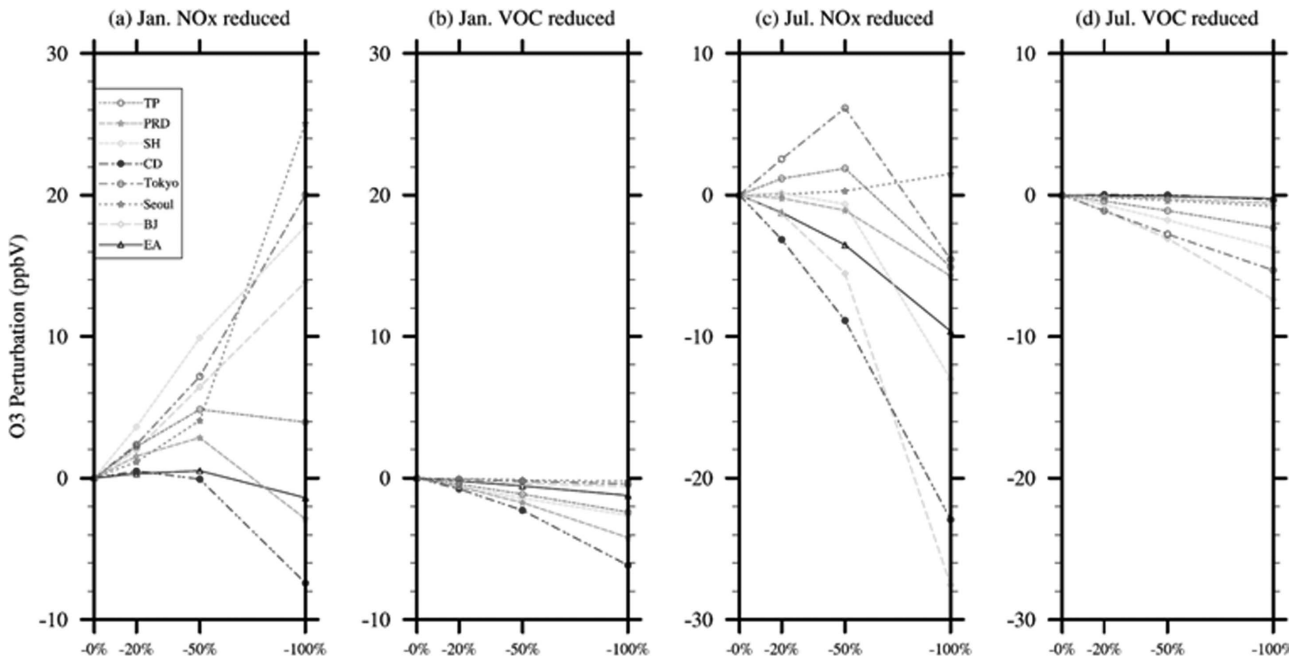

Figure 5. O_3 response (sensitivity cases: base) for EA and seven urban areas, resulted from local emission reduction for (a) NOx and (b) VOC in January, and for (c) NOx and (d) VOC in July 2001.

As shown in Figure 5a, in January, O_3 concentrations in most of the urban areas increase as the anthropogenic NOx emission is reduced 20% at the beginning, implying typical VOC-limited conditions there. However, these urban areas exhibit different results in terms of linearity of O_3 production depending on NOx emission reduction ratios, which could be divided into two groups. The first group includes Seoul, SH, BJ, and Tokyo, where surface O_3 concentrations keep increasing as the anthropogenic NOx emission reduction ratio increases from 20% to 100%. This monotonic increment indicates that these areas have a significant amount of NOx emission and are seriously VOC limited. Jacob et al. (1995) claimed that the nonlinearity of O_3 production response for NOx emission changes in the United States. In this study, however, we find that in EA, for city areas including BJ, SH, and Tokyo, O_3 response is almost linear with respect to NOx reduction. For Seoul, the O_3 concentration increment is even faster when the reduction rate change moves from 50% to 100%. The linearity in these areas indicates the existence of significantly high NOx concentration, which indicates that the production of HNO_3 is the dominant sink for odd hydrogen, and which results in VOC-limited conditions of O_3 production for these urban areas. Under the NOx reduction scenarios, O_3 depletion through titration in nighttime is slowed down in these areas with the removal of anthropogenic NOx emission. The second group includes TP, CD, and PRD, which are also VOC limited in the beginning where O_3 concentrations increase with the NOx emission reduction increases from 20% to 50%, but gradually change to being NOx limited when the reduction rate of NOx continues to increase from 50% to 100%, implying a nonlinear response for O_3 production for these urban areas.

In July, both VOC and NOx reductions lead to an O_3 decrease in most of the areas except for TP, Tokyo, and Seoul, where there is a slight increase in O_3 under 20% and 50% NOx reduction scenarios. TP is located in the south part of EA where temperature and humidity do not differ significantly between January and July, so it is still VOC limited under 20% and 50% NOx reduction scenarios, but when the removal rates continually increase to 100%, TP switches to being NOx limited, which is similar for Tokyo. Seoul shows monotonic increase of O_3 under all NOx reduction scenarios, indicating a highly unbalanced ratio between NOx and VOC emission.

In contrast to the obvious negative correlation between O_3 production and NOx reduction, VOC emission reduction shows a strong linear response for all of the urban areas in both January and July, which is consistent with implications from NOx reduction scenarios indicating the typical VOC-limited conditions in city areas. However, under the same percentage of emission removal rate at 100%, VOC reductions show less significant impact on the change of O_3 than that from NOx. For example, 100% reduction of NOx could result in up to 27.5 ppbv reduction of O_3 in July for BJ, while 100% reduction of VOC only leads to 7.2 ppbv O_3 reduction there. Consequently, anthropogenic NOx contributes more than VOC to the surface O_3 over these areas, but emission control strategy design should be more careful since it is generally impossible to have an actual reduction rate of 100%, and the real reduction may fall into VOC-limited conditions and thus increase the surface O_3 concentration in EA, especially for large metropolitan areas.

Effects of long-range transport

In order to better understand the O_3 change due to NOx reduction, three sensitivity cases are conducted to study the effects of long range transport from EU, SA, and NA under the

HTAP SR3NA, SR3SA, and SR3EU scenarios (Fiore et al., 2009).

Figure 6 illustrates the spatial distribution of monthly average surface O_3 response over EA as a receptor region to 20% reduction of anthropogenic NOx emission from EU, SA, and NA as source regions respectively. All contributions discussed in this section refer to the resulting O_3 change from 20% NOx reduction scenarios in this section. As shown in Figure 6a, long-range transport from EU widely impacts air quality over the whole EA in January, contributing up to 0.34 ppbv of the surface O_3 in the northwest part of EA, and 0.1–0.2 ppbv of the surface O_3 over the northern China plain, Yangtze River Delta (YRD), and the East Ocean along the trace of winter time southeastward monsoon, reflecting its upwind proximity. While in July as shown in Figure 6b, the transport effect from EU is constrained by the summer monsoon from the South China Sea within the northwest part of EA but with a higher contribution of up to 0.60 ppbv for the surface O_3, indicating that the dominant distribution

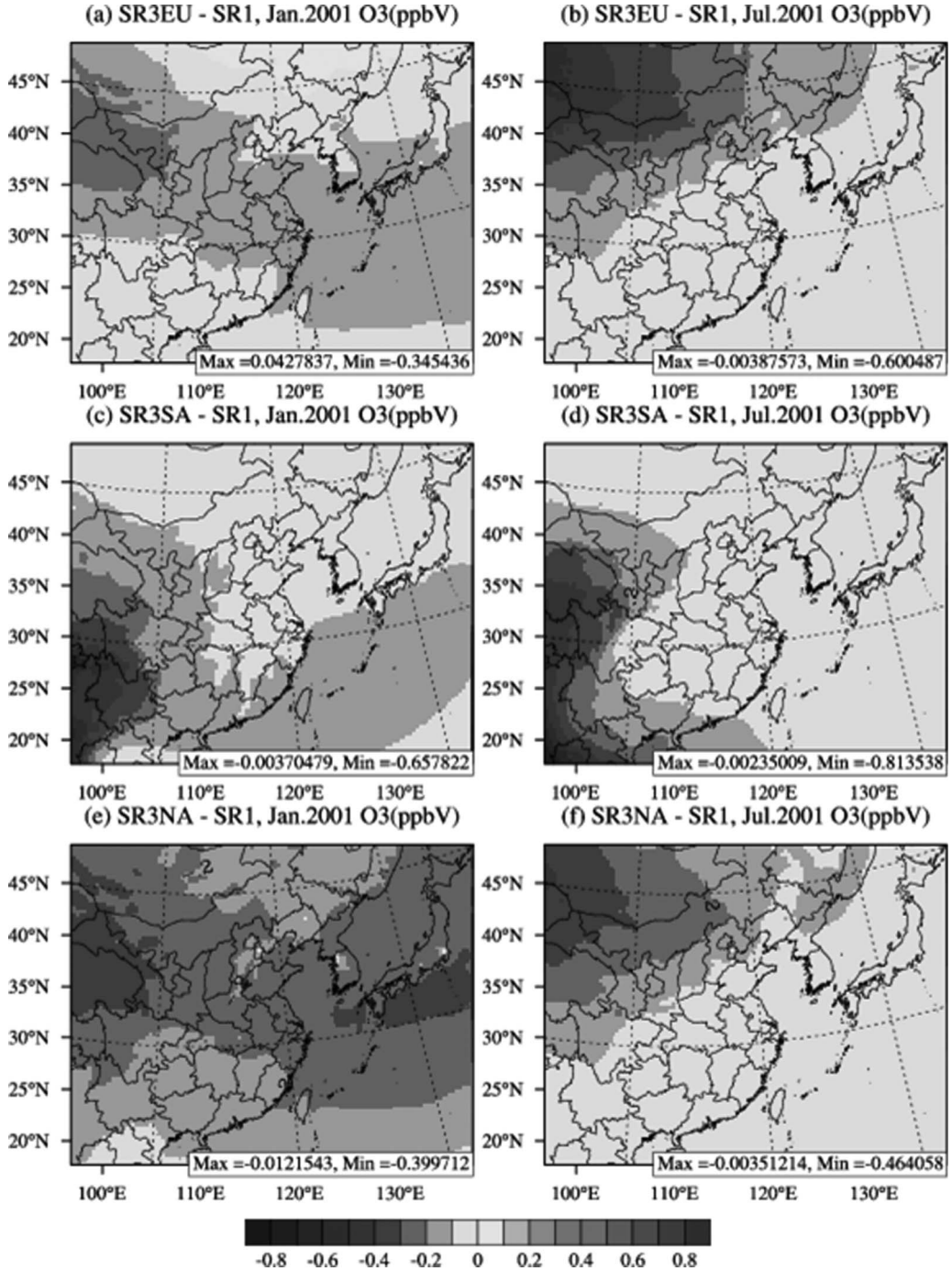

Figure 6. Monthly average O_3 responses over EA as receptor region from 20% reduction of anthropogenic NOx emissions of (a) EU, (c) SA, and (e) NA in January, and (b) EU, (d) SA, and (f) NA in July 2001.

of the transport from EU is mainly determined by the monsoon. Contribution of transport from SA is up to 0.65 ppbv in January and 0.81 ppbv in July, which is constrained in the southwest part of EA by the Himalayas in both months, although the winter monsoon helps to extend the long-range transport along the coast of China. NA has the most significant impact over EA in January, contributing to 0.1–0.3 ppbv for the whole domain. However, the impact of NA is also constrained in the northwest part of EA in the summer time.

In order to examine the relative importance of intercontinental influence from each source region, long-range transport scenarios are also compared with each other and also with the local NOx reduction scenarios to demonstrate the contributions of anthropogenic NOx emissions from local and long-range transport over EA.

Figures 7a, 7b, and 7c illustrate the monthly average and maximum daily O_3 responses for EA and the urban areas under SR3EU, SR3SA, and SR3NA scenarios, respectively. The 20% NOx emission reduction from EU leads to a monthly average surface O_3 decrease of 0.11 ppbv in January and 0.10 ppbv in July over EA, with the maximum daily O_3 changes ranging from 0.23 ppbv in January to 0.28 ppbv in July. This long-range transport effect varies a lot for the seven urban areas. The most affected city is BJ, where resulting monthly average O_3 response is 0.07 ppbv in January and 0.14 ppbv in July. BJ also has the largest maximum daily O_3 response, which is 0.31 ppbv in January and 0.49 ppbv in July, reflecting a downwind location of BJ for both the summer monsoon and the EU emission transport pathway. The transport effect of SA is within the same scale as that of EU, which is 0.13 ppbv in January and 0.11 ppbv in July, but mainly affects the southwest part of EA and is not much affected by the monsoon, resulting in similar O_3 changes in January and July. CD is the most affected urban area by SA in both January and July, where resulting O_3 changes are 0.18 and 0.12 ppbv, respectively, and maximum daily changes reach up to 0.5 and 0.65 ppbv, respectively. Among the three long-range transport scenarios, NA contributes the most as a source region to surface O_3 concentration over EA, and the urban areas in January as the monthly mean O_3 response reached up to 0.23 ppb and 0.5 ppbv for maximum daily response. In July, transport effects over EA from the NA falls into same scale as other source regions. Thus, impacts from intercontinental transport from NA show the largest seasonal variations, especially for the costal areas including SH, PRD, and TP, which are located in the upwind direction in the summer monsoon. For example, the 20% NOx emission reduction of NA leads to 0.38 ppbv daily maximum O_3 decrease for TP in January, while the value is less than 0.01 ppbv in July. O_3 responses caused by NA at the urban areas are generally within the same scale as EA, indicating that the long-range transport effect of NA is widely spread over the whole EA. Intercontinental transport effects are generally stronger in January than that in July, indicating that the wintertime monsoon dominates the imported intercontinental transport of O_3 and its precursors for EA.

Figure 7d shows the monthly average responses under the 20% of local NOx emission reduction scenario (denoted as SR3local). For the entire EA domain, O_3 response to local emission change is 0.32 ppbv in January, which is even smaller than the impact from NA as 0.35 ppbv for daily maxim O_3 response. The impacts from EU and SA are 0.23 and 0.31 ppbv, respectively. Fiore et al. (2009) also reported the annual surface O_3 decrease from a 21-CTM ensemble over EA; values are 0.11, 0.11, and 0.10 ppbv for SR3NA, SR3EU, and SR3SA respectively, and 0.60 ppbv for domestic 20% NOx emission reduction, which is consistent with our CMAQ result, but indicates a smaller significant factor for intercontinental influences based on the global model results. This difference implies uncertainty within the scalability of global model regarding quantifying

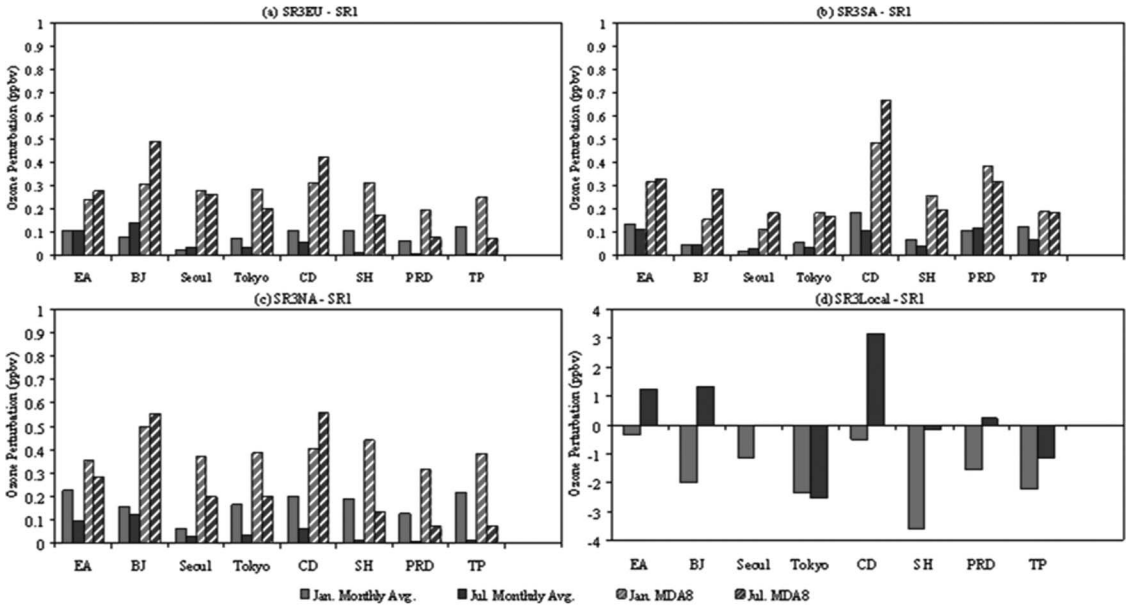

Figure 7. Monthly average and maximum daily O_3 responses under intercontinental transport scenario from (a) EU, (b) SA, and (c) NA, and (d) O_3 perturbation under local 20% NOx emission reduction over EA.

the contributions from source regions, but shows, nevertheless, the comparable impacts as local emission.

For those selected cities in EA, local NOx emission reduction generally has an impact of more than 2 ppbv, while the contributions from outside source regions are usually less than 0.2 ppbv for monthly average and less than 0.7 ppbv for maximum daily, indicating that local emission is the dominant contributor of air pollutants in city areas, but that long-range transport likely contributes greatly to the local pollution as well. For example, SH has less than 0.1 ppbv monthly average O_3 response under local 20% NOx emission reduction in July, while the transport impacts under 20% NOx emission reduction from EU, SA, and NA could reach around 0.2 ppbv for maximum daily O_3 response in SH in July. However, small values for monthly average O_3 response under local NOx emission reduction do not necessarily indicate that local emissions are unimportant, as SH also demonstrated a large daily fluctuation for O_3 response in both January and July, a fluctuation that is not shown in this paper due to its minimal relevance to this study. This indicates the necessity to conduct more comprehensive designed sensitivity simulations over EA to investigate the detailed temporal and spatial variations of local O_3 sensitivities.

This comparison illustrates that although the long-range transport effect is generally smaller in urban areas than the local emission effect, its contribution is still important especially in winter, and this influence could be as high as the impact caused by local emission in certain urban areas, indicating the necessity to take into consideration of long-range transport impact for strategy design since the transport effect could be comparable to the local emission.

Conclusions

In this study, the regional modeling system MM5/CMAQ is applied with 20%, 50%, and 100% emission reduction scenarios of NOx and VOC, respectively and independently, in both January and July 2001 to understand the O_3 formation over EA. Both monthly average and maximum daily O_3 responses are examined for EA and seven urban areas in order to understand the sensitivity and linearity of O_3 production dependence on NOx and VOC, and to provide a theoretical basis for the development of the integrated emission control strategies.

Seasonal variation between January and July suggests that spatial distribution and transport of surface O_3 is strongly affected by monsoon and temperature over EA, resulting in lower O_3 concentration in the north part of EA in January due to less ultraviolet (UV) radiation and southeastward monsoon, and higher O_3 concentration in the same area in July due to increasing temperature and northwestward monsoon.

Investigation of O_3 responses to local NOx emission changes demonstrates that the north part of EA behaves differently from the south part in terms of both seasonal variation and O_3 sensitivity. The northeast part of EA, including north China, South Korea, and Japan, is mainly VOC limited in January and NOx limited in July, although the metropolitan areas including BJ, Seoul, and Tokyo are always VOC limited due to significant amounts of NOx emission from power plants and vehicles. The southeast part is generally NOx limited in both January and July, except for urban areas including PRD and TP, due to large NOx emissions with the seasonal monsoon. The west part of EA is NOx limited in both January and July due to less developed industry and transportation.

Linearity of O_3 response is examined for seven urban areas regarding both NOx and VOC emission changes independently. We find strong negative linearity of O_3 response to NOx reduction in BJ, SH, Seoul, and Tokyo in January, and strong positive linearity of O_3 response to VOC emission reduction in all the seven urban areas in both January and July. Moreover, O_3 responses under 20% of local NOx emission reduction scenarios ranges from 0.7 ppbv in January to -1.2 ppbv in July, which is on a larger scale than that under 20% of VOC emission reduction scenarios, ranging from -0.2 ppbv in January to -0.02 ppbv in July, indicating surface O_3 is more affected by NOx emission than by VOC in EA. However, this assessment should be taken carefully while making emission control strategies, since applicable NOx reduction rates may fall into the VOC-limited condition, which causes surface O_3 increases with decreasing anthropogenic NOx emission.

Intercontinental transport effects from EU, SA, and NA over EA and seven urban areas are also examined under HTAP SR3EU, SR3SA, and SR3NA scenarios, and compared with the local emission reduction scenario to distinguish the contribution of domestic emission from that of long-range transport on surface O_3. As a receptor region, EA benefits from NOx emission reduction in EU, SA, and NA since the surface O_3 concentration decreases in both January and July. The transport effect is found to be higher in January for all source regions than that in July, and the daily maximum O_3 change from long-range transport could be as high as the monthly O_3 change from local NOx emission reduction at the same rate. Contributions from EU and SA are mainly trapped by the dominant monsoon, but NA is found to affect EA, spreading over the entire domain. EU transport effect could reach as far as Japan in January, but is mainly constrained in northwest part of EA in July, while SA transport effect is trapped by the Himalayas in the southwest part of EA. The overall intercontinental transport effect is smaller than the effect from domestic NOx emission reduction by the same rate, which is consistent among the regional model CMAQ and the TF HTAP 21 global CTM ensemble, but could still cause important O_3 changes comparable to local emission in January, and this impact may even reach the same scale as local emission in urban areas. Taking into consideration that global CTMs may underestimate their contributions from source regions due to uncertainties from coarse resolution, the intercontinental transport influences may be larger than that reported by HTAP.

This study illustrates the effectiveness of the regional modeling system MM5/CMAQ to analyze the O_3 sensitivity and linearity over EA, and also examines the impacts of North Hemispheric transport of O_3. Pending is further investigation of the detailed chemical schemes and physical transport processes regarding O_3 and $PM_{2.5}$ as a response to different spatial resolutions at finer scale (12 km), and revealing the seasonal variations through a whole year.

Acknowledgments

This work was supported by the U.S. Environmental Protection Agency under STAR agreement R833370 and the GCAP project. It has not been formally reviewed by the U.S. EPA. The views presented in this document are solely those of the authors and the U.S. EPA does not endorse any products or commercial services mentioned in this publication. We thank the NSF-funded National Institute of Computational Sciences for the use of the Kraken supercomputer on this study. We thank Drs. Daniel Jacob at Harvard University and Rokjin Park currently at Seoul National University for providing the GEOS-Chem outputs. We also thank the Taiwan EPA for providing Taipei observational data.

References

Berntsen, T.K., S. Karlsdottir, and D.A. Jaffe. **1999**. Influence of Asian emissions on the composition of air reaching the northwestern United States. *Geophys. Res. Lett.*. 26(14):2171–2174.

Byun, D.W., and J.K.S. Ching. **1999**. Science Algorithm of the U.S. Environmental Protection Agency (EPA) Models-3 Community Multiscale Air Quality (CMAQ) Modeling System. EPA/600/R-99/030. Washington, DC: U.S. Environmental Protection Agency, Office of Research and Development.

Byun, D., and K.L. Schere. **2006**. Review of the governing equations, computational algorithms, and other components of the Models-3 Community Multiscale Air Quality (CMAQ) modeling system. *Appl. Mech. Rev.* 59 (1–6):51–77.

Cohan, D.S., Y.T. Hu, and A.G. Russell. **2006**. Dependence of ozone sensitivity analysis on grid resolution. *Atmos. Environ*. 40(1):126–135.

Dawson, J.P., S.N. Pandis, and P.J. Adams. **2007**. Sensitivity of ozone to summertime climate in the eastern USA: A modeling case study. *Atmos. Environ.* 41(7):1494–1511.

Dudhia, J.A. 1993. Nonhydrostatic version of the Penn State NCAR Mesoscale Model—Validation tests and simulation of an Atlantic cyclone and coldfront. *Monthly Weather Rev.* 121(5):1493–1513.

Emmerson, K.M., and M.J. Evans. 2009. Comparison of tropospheric gas-phase chemistry schemes for use within global models. *Atmos. Chem. Phys.* 9(5):1831–1845.

Fiore, A.M., F.J. Dentener, O. Wild, C. Cuvelier, M.G. Schultz, P. Hess, C. Textor, M. Schulz, R.M. Doherty, L.W. Horowitz, I.A. MacKenzie, M.G. Sanderson, D.T. Shindell, D.S. Stevenson, S. Szopa, R. Van Dingenen, G. Zeng, C. Atherton, D. Bergmann, I. Bey, G. Carmichael, W.J. Collins, B.N. Duncan, G. Faluvegi, G. Folberth, M. Gauss, S. Gong, D. Hauglustaine, T. Holloway, I.S.A. Isaksen, D.J. Jacob, J.E. Jonson, J.W. Kaminski, T.J. Keating, A. Lupu, E. Marmer, V. Montanaro, R.J. Park, G. Pitari, K.J. Pringle, J.A. Pyle, S. Schroeder, M.G. Vivanco, P. Wind, G. Wojcik, S. Wu, and A. Zuber. 2009. Multimodel estimates of intercontinental source-receptor relationships for ozone pollution. *J. Geophys. Res.* 114(D04301).

Fiore, A.M., D.J. Jacob, I. Bey, R.M. Yantosca, B.D. Field, A.C. Fusco, and J.G. Wilkinson. 2002. Background ozone over the United States in summer: Origin, trend, and contribution to pollution episodes. *J. Geophys. Res.* 107(D15).

Fu, J.S., N.C. Hsu, Y. Gao, K. Huang, C. Li, N.H. Lin, and S.C. Tsay. 2011. A regional chemical transport modeling to identify the influences of biomass burning during 2006 BASE-ASIA. *Atmos. Chem. Phys. Discuss*. 11:3071–3115.

Fu, J.S., D.G. Streets, C.J. Jang, J. Hao, K. He, L. Wang, and Q. Zhang. 2011. Modeling regional/urban ozone and particulate matter in Beijing, China. *J. Air Waste Manage. Assoc.* 59(1):37–44. doi: 10.3155/1047-3289.59.1.37

Hakami, A., M.T. Odman, and A.G. Russell. **2004**. Nonlinearity in atmospheric response: A direct sensitivity analysis approach. *J. Geophys. Res. Atmos*. 109 (D15303).

Heald, C.L., D.J. Jacob, S. Turquety, R.C. Hudman, R.J. Weber, A.P. Sullivan, R.E. Peltier, E.L. Atlas, J.A. de Gouw, C. Warneke, J.S. Holloway, J.A. Neuman, F.M. Flocke, and J.H. Seinfeld. 2006. Concentrations and sources of organic carbon aerosols in the free troposphere over North America. *J. Geophys. Res*. 111(D23S47).

Holloway, T., T. Sakurai, Z. Han, S. Ehlers, S.N. Spak, L.W. Horowitz, G.R. Carmichael, D.G. Streets, Y. Hozumi, H. Ueda, S.U. Park, C. Fung, M. Kajino, N. Thongboonchoo, M. Engardt, C. Bennet, H. Hayami, K. Sartelet, Z. Wang, K. Matsuda, and M. Amann. 2008. MICS-Asia II: Impact of global emissions on regional air quality in Asia. *Atmos. Environ.* 42(15):3543–3561.

Jacob, D.J., L.W. Horowitz, J.W. Munger, B.G. Heikes, R.R. Dickerson, R.S. Artz, and W.C. Keene. 1995. Seasonal transition from NOx- to hydrocarbon-limited conditions for ozone production over the eastern United States in September. *J. Geophys. Res. Atmos*. 100(D5):9315–9324.

Jacob, D.J., J.A. Logan, and P.P. Murti. 1999. Effect of rising Asian emissions on surface ozone in the United States. *Geophys. Res. Lett.* 26(14):2175–2178.

Jaffe, D., T. Anderson, D. Covert, R. Kotchenruther, B. Trost, J. Danielson, W. Simpson, T. Berntsen, S. Karlsdottir, D. Blake, J. Harris, G. Carmichael, and I. Uno. 1999. Transport of Asian air pollution to North America. *Geophys. Res. Lett.* 26(6):711–714.

Kain, J.S., and J.M. Fritsch. 1993. Convective parameterization for mesoscale models: The Kain–Fritsch scheme. In *The Representation of Cumulus Convection in Numerical Models*; Emanuel, K.A., Raymond, D.J., Eds.; Boston, MA: American Metrological Society.

Kim, Y., J.S. Fu, and T.L. Miller. 2010. Improving ozone modeling in complex terrain at a fine grid resolution—Part : Influence of schemes in MM5 on daily maximum 8-hour ozone concentrations and RRF (relative reduction factors) for SIPs in the nonattainment areas. *Atmos. Environ*. 44:2116–2124.

Lam, Y.F., and J.S. Fu. 2009. A novel downscaling technique for the linkage of global and regional air quality modeling. *Atmos. Chem. Phys.* 9(23):9169–9185.

Lam, Y.F., and J.S. Fu. 2010. Corrigendum to "Novel downscaling technique for the linkage of global and regional air quality modeling" (vol 9, pg 9169, 2009). *Atmos. Chem. Phys*. 10(8):4013–4031.

Li, L., C.H. Chen, J.S. Fu, C. Huang, D.G. Streets, H.Y. Huang, G.F. Zhang, Y.J. Wang, C.J. Jang, H.L. Wang, Y.R. Chen, and J.M. Fu. 2011. Air quality and emissions in the Yangtze River Delta, China. *Atmos. Chem. Phys.* 11 (4):1621–1639.

Lin, M., T. Holloway, T. Oki, D.G. Streets, and A. Richter. 2008. Mechanisms controlling surface ozone over East Asia: A multiscale study coupling regional and global chemical transport models. *Atmos. Chem. Phys. Discuss*. 8:20239–20281.

Liu, Y., I.S.A. Isaksen, J.K. Sundet, J.H. He, and P. Yan. 2004. NOx change over China and its influences. *Adv. Atmos. Sci*. 21(1):132–140.

Luo, C., J.C.S. John, X.J. Zhou, K.S. Lam, T. Wang, and W.L. Chameides. 2000. A nonurban ozone air pollution episode over eastern China: Observations and model simulations. *J. Geophys. Res. Atmos*. 105(D2):1889–1908.

National Research Council. 1991. *Rethinking the Ozone Problem in Urban and Regional Air Pollution*. Washington, DC: National Academies Press.

Reisner, J., R.M. Rasmussen, and R.T. Bruintjes. 1998. Explicit forecasting of supercooled liquid water in winter storms using the MM5 mesoscale model. *Q. J. R. Meteorol. Soc*. 124(548):1071–1107.

Sillman, S. 1995. The use of NOx, H_2O_2, and HNO_3 as indicators for ozone–NOx–hydrocarbon sensitivity in urban locations. *J. Geophys. Res.* 100 (D7):14175–14188.

Sillman, S. 1999. The relation between ozone, NOx and hydrocarbons in urban and polluted rural environments. *Atmos. Environ*. 33(12):1821–1845.

Sillman, S., and D.Y. He. 2002. Some theoretical results concerning O3-NOx-VOC chemistry and NOx-VOC indicators. *J. Geophys. Res.* 107(D22).

So, K.L., and T. Wang. 2003. On the local and regional influence on ground-level ozone concentrations in Hong Kong. *Environ. Pollut*. 123(2):307–317.

Streets, D.G., T.C. Bond, G.R. Carmichael, S.D. Fernandes, Q. Fu, D. He, Z. Klimont, S.M. Nelson, N.Y. Tsai, M.Q. Wang, J.H. Woo, and K.F. Yarber, 2003. An inventory of gaseous and primary aerosol emissions in Asia in the year 2000. *J. Geophys. Res.* 108(D21).

Streets, D.G., J.S. Fu, C.J. Jang, J.M. Hao, K.B. He, X.Y. Tang, Y.H. Zhang, Z.F. Wang, Z.P. Li, Q. Zhang, L.T. Wang, B.Y. Wang, and C. Yu. 2007. Air quality during the 2008 Beijing Olympic Games. *Atmos. Environ.* 41 (3):480–492.

Walcek, C.J., and N.M. Aleksic. 1998. A simple but accurate mass conservative, peak-preserving, mixing ratio bounded advection algorithm with Fortran code. *Atmos. Environ.* 32(22):3863–3880.

Wang, X.M., G. Carmichael, D.L. Chen, Y.H. Tang, and T.J. Wang. 2005. Impacts of different emission sources on air quality during March 2001 in the Pearl River Delta (PRD) region. *Atmos. Environ*. 39(29):5227–5241.

Wesely, M.L. 1989. Parameterization of surface resistances to gaseous dry deposition in regional-scale numerical-models. *Atmos. Environ.* 23(6):1293–1304.

Willmont, C.J. 1981. On the validation of models. *Phys. Geogr.* 2:168–194.

Woo, J., D. Streets, G. Carmichael, J. Dorwart, N. Thongboonchoo, S. Guttikunda, and Y. Tang, 2002. Development of the Emission Inventory System for supporting TRACE-P and ACE-Asia field experiments. *Air Pollution Modelling and Its Application*. XV: 527–528. Louvain-la-Neuve, Belgium.

Wu, S.L., B.N. Duncan, D.J. Jacob, A.M. Fiore, and O. Wild. 2009. Chemical nonlinearities in relating intercontinental ozone pollution to anthropogenic emissions. *Geophys. Res. Lett*. 36.

Xing, J., S.X. Wang, C. Jang, Y. Zhu, and J.M. Hao. 2011. Nonlinear response of ozone to precursor emission changes in China: A modeling study using response surface methodology. *Atmos. Chem. Phys.* 11(10):5027–5044.

Xu, X., W. Lin, T. Wang, P. Yan, J. Tang, Z. Meng, and Y. Wang. 2008. Long-term trend of surface ozone at a regional background station in eastern China 1991–2006: Enhanced variability. *Atmos. Chem. Phys.* 8(10):2595–2607.

Yamaji, K., I. Uno, and H. Irie. 2012. Investigating the response of East Asian ozone to Chinese emission changes using a linear approach. *Atmos. Environ.* 55:475–482.

Zhang, D., and R.A.A. Anthes. 1982. High-resolution model of the planetary boundary layer—Sensitivity tests and comparisons with SESAME-79 data. *J. Appl. Meteorol.* 21(11):1594–1609.

Zhang, Y.N., Y.R. Xiang, L.Y. Chan, C.Y. Chan, X.F. Sang, R. Wang, and H.X. Fu. 2011. Procuring the regional urbanization and industrialization effect on ozone pollution in Pearl River Delta of Guangdong, China. *Atmos. Environ*. 45(28):4898–4906.

About the Authors

Joshua S. Fu is an associate professor at the Department of Civil Engineering, University of Tennessee, in Knoxville.

Xinyi Dong and **Yang Gao** are graduate students at the Department of Civil Engineering, University of Tennessee, in Knoxville.

David C. Wong is a computational scientist at the Atmospheric Modeling and Analysis Division, U.S. Environmental Protection Agency, in Research Triangle Park, NC.

Yun Fat Lam is a visiting assistant professor in the School of Energy and Environment, City University of Hong Kong, in Hong Kong, China.